

Direct observation of the charge carrier concentration in organic field-effect transistors by electron spin resonance

Hisaaki Tanaka,^{1,a)} Shun-ichiro Watanabe,¹ Hiroshi Ito,¹ Kazuhiro Marumoto,² and Shin-ichi Kuroda¹

¹Department of Applied Physics, Nagoya University, Chikusa, Nagoya 464-8603, Japan

²Institute of Materials Science, University of Tsukuba, Tsukuba 305-8573, Japan

(Received 27 December 2008; accepted 24 February 2009; published online 13 March 2009)

Charge carrier concentration in operating field-effect transistor (FET) of regioregular poly(3-hexylthiophene) has been directly determined by electron spin resonance (ESR). ESR signals of field-induced polarons are observed around $g=2.003$ under the application of negative gate-source voltage (V_{gs}). Upon applying drain-source voltage (V_{ds}), ESR intensity decreases linearly in the low V_{ds} region, reaching to about 50% of the initial intensity at the pinch-off point ($V_{ds} \cong V_{gs}$). For larger absolute values of V_{ds} , it becomes nearly V_{ds} independent. These behaviors are well explained by the change in the carrier concentration obtained by the FET theory using gradual channel approximation. © 2009 American Institute of Physics. [DOI: 10.1063/1.3100193]

Organic field-effect transistors (FETs) have been attracting considerable attention owing to their structural flexibility, large area coverage, and low-cost processing.¹⁻³ Light-emitting properties of organic FETs have also been reported.^{4,5} The studies of charge carriers in these devices are of fundamental importance in understanding the basic physical processes, such as carrier injection, accumulation, and transport, and hence, may contribute to the formulation of the design principle of highly efficient devices. However, intrinsic transport properties in the devices tend to be masked due to the molecular disorders at the device interfaces. Thus far, spectroscopic studies such as charge modulation spectroscopy⁶ or infrared spectroscopy⁷ have been applied to observe the field-induced charge carriers in metal-insulator-semiconductor (MIS) devices of semiconducting polymers with high mobilities, such as regioregular poly(3-hexylthiophene) (RR-P3HT) [Fig. 1(a)] or poly(3-octylthiophene) (RR-P3OT).^{2,3} These studies demonstrate that the injected charge carriers are polarons, which are typical nonlinear excitations in the conjugated polymers.⁸ More recently, spectroscopic imaging of the carriers in the channel region of FETs during the device operation has been reported for the devices of RR-P3HT (Ref. 9) or pentacene.¹⁰

On the other hand, direct determination of the injected carrier concentration is also the key issue to characterize the device properties of the organic FETs. According to the standard FET theory, the change in the carrier concentration in the FET channel region is induced by the application of the drain-source voltage (V_{ds}) together with the gate-source voltage (V_{gs}), which dominates the output characteristics of the devices.¹¹ The surface potential profile of operating RR-P3HT FETs has been reported by using Kelvin probe force microscopy.¹² The observed potential profile has shown a clear change between the linear region ($V_{gs} > V_{ds}$) and the saturation (or superlinear) region ($V_{gs} < V_{ds}$) of the device, which may be consistent with the prediction of the standard FET theory in the first approximation. There have been, however, no direct observations of the change in the total charge

carrier concentration in the operating FET channel region, corresponding to the change in the potential profile. Such information, if obtained by a microscopic method, can provide a direct evidence for the microscopic origin of the field-induced charge carriers in operating FETs, which should be associated with the organic molecules at the device interface. Electron spin resonance (ESR) spectroscopy is a particularly suitable method for this purpose since the direct observations of the field-induced charge carriers in organic devices have been reported for the MIS diodes of RR-P3HT and RR-P3OT¹³⁻¹⁵ or for the FET devices of pentacene in the absence of drain-source voltages.^{16,17}

In this letter, we report on the ESR measurements of the concentration of the field-induced charge carriers in the FET devices of RR-P3HT during the device operation. The charge carriers are shown to be the polarons of RR-P3HT from the observed g -values around 2.003 of field-induced ESR signals. The concentration of the charge carriers obtained from the ESR intensity decreased linearly by applying V_{ds} up to the pinch-off point ($V_{ds} \cong V_{gs}$), whereas it became independent of V_{ds} for the region of $|V_{ds}| > |V_{gs}|$. These behaviors showed an excellent agreement with the change in the carrier concentration expected from the standard FET theory using gradual channel approximation.

Schematic illustration of the FET device is shown in Fig. 1(a) together with the chemical structure of RR-P3HT. We adopted the top-contact geometry with the channel length

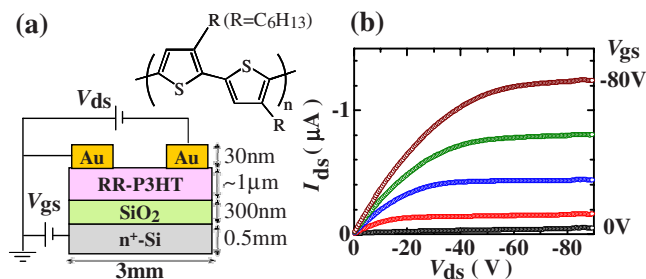


FIG. 1. (Color online) (a) Schematic illustration of the FET device structure. The chemical structure of RR-P3HT is also shown. (b) Output characteristic of the present FET. The gate-source voltage varies from 0 to -80 V (-20 V step).

^{a)}Electronic mail: htanaka@nuap.nagoya-u.ac.jp.

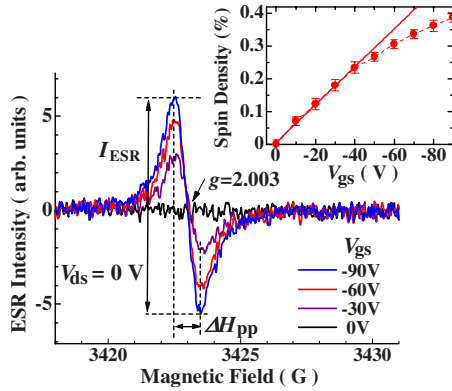


FIG. 2. (Color online) First-derivative field-induced ESR signals obtained for various V_{gs} values without applying V_{ds} . The external magnetic field is perpendicular to the substrate. Inset shows the V_{gs} dependence of the induced spin concentration per thiophene monomer unit. The solid line shows the linear guide to the eye.

and channel width being 1 and 13 mm, respectively. The devices were fabricated on n^+ -Si substrates with SiO_2 gate insulators¹⁵ instead of quartz glass substrates with aluminum gates and Al_2O_3 gate insulators used in the earlier ESR studies of field-effect devices.^{13,14,16} An n^+ -Si wafer (10–20 Ω cm, (100) axis, and 0.5 mm thick) was cut out to 3×30 mm² rectangular substrates. A relatively high value of the surface resistivity of the wafer was chosen so that the deterioration of the quality factor (Q -factor) of the ESR cavity is minimized. The thickness of SiO_2 layer was about 300 nm. RR-P3HT (Aldrich, head-to-tail ratio of >98.5%) was used as purchased. Other details of the device fabrication are described elsewhere.^{13–15} FET characteristics were measured by using Keithley 2400 and 6487 source measure units to apply V_{gs} and V_{ds} , respectively. ESR measurements were performed by using a Bruker E-500 spectrometer equipped with a TE_{011} cylindrical cavity. ESR signals of the field-induced polarons were obtained by subtracting the background ESR signal at $V_{gs} = +30$ V from those recorded at $V_{gs} < 0$ V.^{13–15} The spin concentration was determined from the twice-integration of the first-derivative ESR signal calibrated by that of $\text{CuSO}_4 \cdot 5\text{H}_2\text{O}$.

Figure 1(b) shows the output characteristics of the present device. We have obtained a standard behavior exhibiting clearly the linear and saturation regions. In the saturation region of $|V_{ds}| \geq |V_{gs} - V_{th}|$, I_{ds} is formulated as¹¹

$$I_{ds} = \left(\frac{C_i W}{2L} \right) \mu (V_{gs} - V_{th})^2, \quad (1)$$

where C_i , μ , and V_{th} are the capacitance of the insulator, the field-effect mobility, and the threshold voltage, respectively. With the channel length $L = 1$ mm and the channel width $W = 13$ mm, the parameter values are obtained as $\mu = 2 \times 10^{-3}$ cm²/V s and $V_{th} \approx +10$ V.

Figure 2 shows V_{gs} dependence of the first-derivative ESR signal obtained with shortening the source and drain electrodes. In this case, FET structure is identical to a MIS structure. The g -value ($g = 2.003$), which is determined from the resonance field, and the peak-to-peak linewidth ΔH_{pp} ($\Delta H_{pp} = 1.0$ G) of the ESR signals defined in Fig. 2 agree well with our previous results for the MIS devices,^{13–15} indicating that the injected carriers are positive polarons of RR-P3HT associated with unpaired π -electrons. The ESR

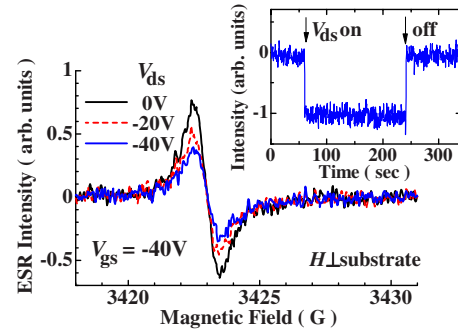


FIG. 3. (Color online) Field-induced ESR signals obtained under the application of V_{ds} together with V_{gs} with the external magnetic field perpendicular to the substrate. Inset shows the time response of the field-induced ESR intensity upon the application of V_{ds} .

signal increases as $|V_{gs}|$ increases. The inset shows the V_{gs} dependence of the induced spin concentration.^{14,15} That is, the spin concentration, shown as the spin density per thiophene monomer unit, starts to linearly increase as $|V_{gs}|$ increases. On the other hand, the spin density tends to saturate above about 0.2% for higher $|V_{gs}|$ values ($V_{gs} < -40$ V). This indicates the formation of spinless charged states such as bipolarons. Such spin saturation has not been observed in pentacene cases,^{16,17} showing that the formation of spinless state is an intrinsic property of the polymer chain.

On the other hand, ESR signal decreases clearly by applying V_{ds} together with V_{gs} without changing g -values and linewidth, as shown in Fig. 3. Here, V_{gs} is fixed at -40 V, where the formation of bipolaron is negligible, as shown in the inset of Fig. 2. In this case, the ESR signal probes all the induced carriers (polarons) in the FET channel. As shown in the inset of Fig. 3, change in the ESR intensity upon the application of V_{ds} occurs within the time resolution of the present ESR measurements (~ 300 ms). Incidentally, no change in the linewidth, observed for the ESR signal during the application of V_{ds} , is consistent with the fact that the carrier velocity estimated from the carrier mobility was low enough so that the motional narrowing effect of the ESR linewidth did not occur. More detailed discussion of such motional effect, however, is beyond the scope of this work.

Figure 4(a) shows V_{ds} dependence of the ESR intensity,

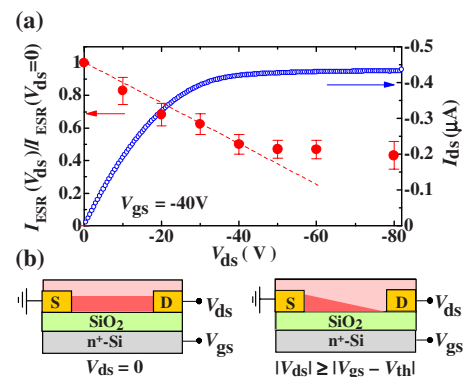


FIG. 4. (Color online) (a) V_{ds} dependence of the ESR intensity normalized by the value at $V_{ds} = 0$ under the application of $V_{gs} = -40$ V (closed circles). The drain current of the FET is also shown for comparison (open circles). The broken line shows the linear guide to the eye. (b) Schematic illustrations of the carrier concentration in the FET channel region for the cases of $V_{ds} = 0$ and $|V_{ds}| \geq |V_{gs} - V_{th}|$.

I_{ESR} defined in Fig. 3, normalized by the value at $V_{\text{ds}}=0$. The ESR intensity decreases linearly by applying V_{ds} in the low V_{ds} region and it reaches about 50% of the initial intensity at $V_{\text{ds}}=-40$ V, where $V_{\text{ds}} \cong V_{\text{gs}}$ is satisfied. On the other hand, I_{ESR} becomes nearly V_{ds} independent in the region of $|V_{\text{ds}}| \geq |V_{\text{gs}}|$. These behaviors are well explained by the change in the carrier concentration in the channel region expected by the FET theory using gradual channel approximation as discussed below.

By applying V_{ds} , a gradient of the carrier concentration is induced, reflecting the potential distribution in the FET channel. In the gradual channel approximation, a linear change in the carrier concentration is assumed, as schematically illustrated in Fig. 4(b) for the cases of $V_{\text{ds}}=0$ and $|V_{\text{ds}}| \geq |V_{\text{gs}} - V_{\text{th}}|$ of the bottom contact geometry.¹⁸ In the linear region of $|V_{\text{ds}}| < |V_{\text{gs}} - V_{\text{th}}|$, the total carrier concentration is described as¹¹

$$Q = \left\{ \frac{1}{2} V_{\text{ds}} - (V_{\text{gs}} - V_{\text{th}}) \right\} LWC_i. \quad (2)$$

This equation directly predicts the linear change in the carrier concentration with respect to V_{ds} , as is actually observed in the present ESR measurements, as shown by closed circles in Fig. 4(a). For the saturation region, the carrier concentration no longer changes from the value at the pinch-off point ($V_{\text{ds}} = V_{\text{gs}} - V_{\text{th}}$); $Q = -(1/2)(V_{\text{gs}} - V_{\text{th}})LWC_i$.¹¹ The important point is that the carrier concentration at the pinch-off point is exactly 50% of that at $V_{\text{ds}}=0$, which is easily derived from Eq. (2). This behavior is *indeed* confirmed in the present study at $V_{\text{ds}}=-40$ V as already pointed out by using Fig. 4(a). Here, V_{th} is assumed to be nearly zero from the V_{gs} dependence of the spin concentration shown in the inset of Fig. 2, since the accuracy of V_{th} is higher in this case than that obtained from FET output characteristics.

As seen from Fig. 4(a), the pinch-off point for the ESR intensity variation and that of the FET output currents, shown by open circles, nearly coincide. Therefore, we have demonstrated directly the change in the carrier concentration in the FET channel region, which agrees well with the FET theory. The above obtained drain-source voltage effect on the field-induced ESR signal has also been confirmed in the FET devices with different channel lengths. Also, similar results have been confirmed in the FET devices of RR-P3HT fabricated on Al_2O_3 gate insulators. These results indicate that the presently obtained results represent common features of the operating FETs.

In summary, the V_{ds} dependence of the charge carrier concentration in the channel region of operating organic FET devices of RR-P3HT has been microscopically clarified through the ESR method. The results are well described by

the FET theory with gradual channel approximation. The presently obtained results demonstrate the potential of the ESR method in accurately obtaining the concentration of the charge carriers in operating FETs and hence the extension to various organic FET devices including single crystalline ones¹⁹ may be useful in providing microscopic information of the active layers of organic FETs.

This work was partially supported by Grant-in-Aid for Scientific Research (Grant No. 17340094) and for Science Research in a Priority Area ‘‘Super-Hierarchical Structures’’ (Grant No. 17067007) from the Ministry of Education, Culture, Sports, Science and Technology of Japan.

¹C. D. Dimitrakopoulos and P. R. L. Malenfant, *Adv. Mater. (Weinheim, Ger.)* **14**, 99 (2002).

²H. Sirringhaus, P. J. Brown, R. H. Friend, M. M. Nielsen, K. Bechgaard, B. M. W. Langeveld-Voss, A. J. H. Spiering, R. A. J. Janssen, E. W. Meijer, P. Herwig, and D. M. de Leeuw, *Nature (London)* **401**, 685 (1999).

³M. Surin, Ph. Leclere, R. Lazzaroni, J. D. Yuen, G. Wang, D. Moses, A. J. Heeger, S. Cho, and K. Lee, *J. Appl. Phys.* **100**, 033712 (2006).

⁴A. Hepp, H. Heil, W. Weise, M. Ahles, R. Schmechel, and H. von Seggern, *Phys. Rev. Lett.* **91**, 157406 (2003).

⁵F. Cicoira and C. Santato, *Adv. Funct. Mater.* **17**, 3421 (2007).

⁶P. J. Brown, H. Sirringhaus, M. Harrison, M. Shkunov, and R. H. Friend, *Phys. Rev. B* **63**, 125204 (2001).

⁷Y. Furukawa, J. Yamamoto, D. C. Cho, and T. Mori, *Macromol. Symp.* **205**, 9 (2004).

⁸A. J. Heeger, S. Kivelson, J. R. Schrieffer, and W. P. Su, *Rev. Mod. Phys.* **60**, 781 (1988).

⁹Z. Q. Li, G. M. Wang, N. Sai, D. Moses, M. C. Martin, M. Di Ventra, A. J. Heeger, and D. N. Basov, *Nano Lett.* **6**, 224 (2006).

¹⁰T. Manaka, E. Lim, R. Tamura, and M. Iwamoto, *Nat. Photonics* **1**, 581 (2007).

¹¹S. M. Sze, *Physics of Semiconductor Devices* (Wiley, New York, 1969).

¹²L. Bürgi, H. Sirringhaus, and R. H. Friend, *Appl. Phys. Lett.* **80**, 2913 (2002).

¹³K. Marumoto, Y. Muramatsu, S. Ukai, H. Ito, and S. Kuroda, *J. Phys. Soc. Jpn.* **73**, 1673 (2004).

¹⁴K. Marumoto, Y. Muramatsu, Y. Nagano, T. Iwata, S. Ukai, H. Ito, S. Kuroda, Y. Shimoi, and S. Abe, *J. Phys. Soc. Jpn.* **74**, 3066 (2005).

¹⁵S. Watanabe, K. Ito, H. Tanaka, H. Ito, K. Marumoto, and S. Kuroda, *Jpn. J. Appl. Phys., Part 2* **46**, L792 (2007).

¹⁶K. Marumoto, S. Kuroda, T. Takenobu, and Y. Iwasa, *Phys. Rev. Lett.* **97**, 256603 (2006).

¹⁷H. Matsui, T. Hasegawa, Y. Tokura, M. Hiraoka, and T. Yamada, *Phys. Rev. Lett.* **100**, 126601 (2008).

¹⁸The present measurements have been done by adopting the top-contact geometry, where we have to consider the carriers accumulated under the drain and source electrodes in addition to those accumulated in the channel region shown in Fig. 4(b). However, the total carrier concentration is formulated by the same form as Eq. (2) even for the top-contact FETs within the framework of the gradual channel approximation by adjusting the channel length L to include the widths of the electrodes. Thus, there are no ambiguities arising from the geometry of the device in the present study.

¹⁹M. E. Gershenson, V. Podzorov, and A. F. Morpurgo, *Rev. Mod. Phys.* **78**, 973 (2006).